Enzyme Catalysis and Regulation:

ATP-driven Reduction by Dark-operative Protochlorophyllide Oxidoreductase from *Chlorobium tepidum* Mechanistically Resembles Nitrogenase Catalysis

Markus J. Bröcker, Simone Virus, Stefanie Ganskow, Peter Heathcote, Dirk W. Heinz, Wolf-Dieter Schubert, Dieter Jahn and Jürgen Moser

J. Biol. Chem. 2008, 283:10559-10567.
doi: 10.1074/jbc.M708010200 originally published online February 5, 2008

THE JOURNAL OF BIOLOGICAL CHEMISTRY VOL. 283, NO. 16, pp. 10559–10567, April 18, 2008

ATP-driven Reduction by Dark-operative Protochlorophyllide Oxidoreductase from *Chlorobium tepidum* Mechanistically Resembles Nitrogenase Catalysis*[S]

Received for publication, September 25, 2007, and in revised form, January 29, 2008 Published, JBC Papers in Press, February 5, 2008, DOI 10.1074/jbc.M708010200

Markus J. Bröcker[‡], Simone Virus[‡], Stefanie Ganskow[§], Peter Heathcote[¶], Dirk W. Heinz[‖], Wolf-Dieter Schubert[‖], Dieter Jahn[‡], and Jürgen Moser[‡1]

From the [‡]Institute of Microbiology, Technical University Braunschweig, Spielmannstrasse 7, D-38106 Braunschweig, Germany, the [§]Institut für Biologie, Humboldt Universität zu Berlin, Chausseestrasse 117, D-10115 Berlin, Germany, the [¶]School of Biological Sciences, Queen Mary and Westfield College, Mile End Road, London E1 4NS, United Kingdom, and the [‖]Division of Structural Biology, Helmholtz-Centre for Infection Research, Inhoffenstraße 7, D-38124 Braunschweig, Germany

During chlorophyll and bacteriochlorophyll biosynthesis in gymnosperms, algae, and photosynthetic bacteria, dark-operative protochlorophyllide oxidoreductase (DPOR) reduces ring D of aromatic protochlorophyllide stereospecifically to produce chlorophyllide. We describe the heterologous overproduction of DPOR subunits BchN, BchB, and BchL from *Chlorobium tepidum* in *Escherichia coli* allowing their purification to apparent homogeneity. The catalytic activity was found to be 3.15 nmol min^{-1} mg^{-1} with K_m values of 6.1 μM for protochlorophyllide, 13.5 μM for ATP, and 52.7 μM for the reductant dithionite. To identify residues important in DPOR function, 21 enzyme variants were generated by site-directed mutagenesis and investigated for their metal content, spectroscopic features, and catalytic activity. Two cysteine residues (Cys^{97} and Cys^{131}) of homodimeric $BchL_2$ are found to coordinate an intersubunit [4Fe-4S] cluster, essential for low potential electron transfer to $(BchNB)_2$ as part of the reduction of the protochlorophyllide substrate. Similarly, Lys^{10} and Leu^{126} are crucial to ATP-driven electron transfer from $BchL_2$. The activation energy of DPOR electron transfer is 22.2 kJ mol^{-1} indicating a requirement for 4 ATP per catalytic cycle. At the amino acid level, BchL is 33% identical to the nitrogenase subunit NifH allowing a first tentative structural model to be proposed. In $(BchNB)_2$, we find that four cysteine residues, three from BchN (Cys^{21}, Cys^{46}, and Cys^{103}) and one from BchB (Cys^{94}), coordinate a second intersubunit [4Fe-4S] cluster required for catalysis. No evidence for any type of molybdenum-containing cofactor was found, indicating that the DPOR subunit BchN clearly differs from the homologous nitrogenase subunit NifD. Based on the available data we propose an enzymatic mechanism of DPOR.

Protochlorophyllide (Pchlide)[2] is a central metabolite for the biosynthesis of chlorophylls (Chl) and bacteriochlorophylls (bChl). In photosynthetic organisms two distinct enzymes catalyze the stereospecific reduction of ring D of the aromatic Pchlide to form chlorophyllide (Chlide) (1–3) (Fig. 1). The first enzyme is the light-dependent Pchlide oxidoreductase (LPOR; NADPH Pchlide oxidoreductase, EC 1.3.1.33). To achieve the chemically difficult reduction of the aromatic ring system, the complex of monomeric LPOR and substrate Pchlide must absorb light energy prior to NADPH-dependent reduction (4–6) making LPOR a dominant player in the light-dependent greening of flowering plants (angiosperms) (7, 8). The second Pchlide-reducing enzyme is the light-independent (dark) Pchlide oxidoreductase (DPOR), which shares no amino acid sequence homology to the LPOR system. It consumes ATP to drive the production of Chlide. Some anoxygenic bacteria only encode DPOR (9), whereas angiosperms exclusively produce LPOR. Cyanobacteria, algae, and gymnosperms possess both LPOR and DPOR (1). DPOR enables these organisms to synthesize bChl or Chl in the dark.

In bChl-synthesizing organisms the genes *bchN*, *bchB*, and *bchL* encode the three subunits of DPOR. In Chl-synthesizing organisms the corresponding genes are known as *chlN*, *chlB*, and *chlL* (10–12). Protein subunits of DPOR share significant amino acid sequence similarity with NifD, NifK, and NifH, the three subunits of nitrogenase. Among the subunits of DPOR, BchL is most similar to its counterpart NifH sharing 33% amino acid sequence identity (13). The remaining two DPOR subunits BchN and BchB are similarly related to NifD and NifK, although sequence identities at ~15% (for both comparisons) are not as pronounced (14).

The well characterized nitrogenase protein complex consists of homodimeric Fe-dinitrogenase reductase (Fe-protein, $NifH_2$) and tetrameric MoFe-protein complex ($(NifD/NifK)_2$) responsible for the reduction of dinitrogen to ammonia (15–17). $NifH_2$ binds an intersubunit [4Fe-4S] redox cluster symmetrically coordinated by two cysteine residues (Cys^{97} and Cys^{132}, *Azotobacter vinelandii* numbering) from each NifH subunit. This redox center is required for the ATP-driven

* This work was supported by the Deutsche Forschungsgemeinschaft. The costs of publication of this article were defrayed in part by the payment of page charges. This article must therefore be hereby marked "*advertisement*" in accordance with 18 U.S.C. Section 1734 solely to indicate this fact.

[S] The on-line version of this article (available at http://www.jbc.org) contains supplemental Fig. S1.

[1] To whom correspondence should be addressed. Tel.: 49-531-391-5808; Fax: 49-531-391-5854; E-mail: j.moser@tu-bs.de.

[2] The abbreviations used are: Pchlide, protochlorophyllide; bChl, bacteriochlorophyll; Chl, chlorophyll; Chlide, chlorophyllide; GST, glutathione *S*-transferase; ICP-MS, inductively coupled plasma mass spectrometry; HPLC, high pressure liquid chromatography; LPOR, light-dependent protochlorophyllide oxididoreductase; DPOR, dark-operative protochlorophyllide oxidoreductase.

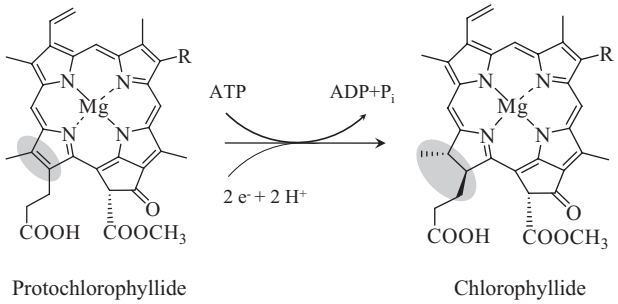

FIGURE 1. **Reduction of the aromatic ring system of Pchlide by DPOR.** Ring D is stereospecifically reduced in the presence of an electron donor and ATP. *R* is either a vinyl or an ethyl moiety.

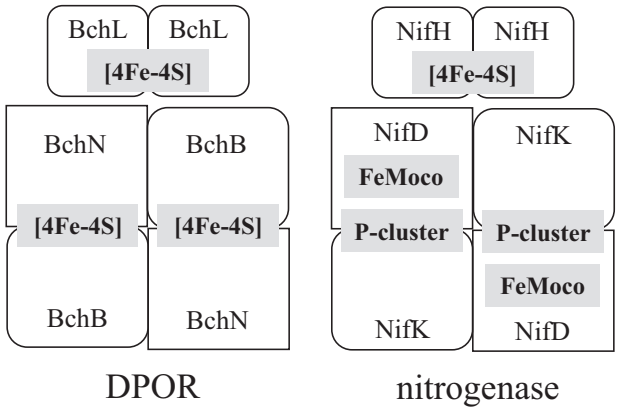

FIGURE 2. **Schematic model of DPOR and nitrogenase.** The inferred subunit and cofactor composition of DPOR is indicated and compared with that of nitrogenase.

transfer of electrons from ferredoxin to $(NifD/NifK)_2$. These two cysteines are perfectly conserved in all BchL/ChlL protein sequences (10).

The tetrameric $(NifD/NifK)_2$ MoFe complex bears two types of metallocenters, an [8Fe-7S] cluster (P-cluster) located at the interface of the NifD and NifK subunits and a [1Mo-7Fe-9S-1homocitrate] or MoFe cofactor located within each NifD subunit (Fig. 2). The P-cluster is thought to mediate electron transfer from $NifH_2$ to the MoFe cofactor, where final dinitrogen reduction takes place (18).

BchN and BchB together contain only four highly conserved cysteines, compared with six cysteines coordinating the [8Fe-7S] P-cluster in NifD/NifK. Three are found in BchN (Cys^{21}, Cys^{46}, Cys^{103}, *C. tepidum* numbering) and one in BchB (Cys^{94}). A bridging Fe-S center, although presumably smaller than the P-cluster, may thus be located at the interface of BchN and BchB. Residues involved in MoFe cofactor binding in NifD are not conserved in BchN implying that this part of dinitrogen reduction does not have a counterpart in reduction of Pchlide.

Several protein complexes of dinitrogenase reductase and the MoFe-protein have been trapped using AlF_4^- or BeF_3^- together with Mg-ADP, or by deleting Leu^{127} in the ATP-binding motif of $NifH_2$ (19). The [4Fe-4S] cluster of $NifH_2$ has, moreover, been shown to be a better reductant when in complex with the MoFe-protein, than in its uncomplexed form (20). These findings indicate that the BchL subunits of DPOR may similarly catalyze an ATP-driven transfer of electrons from a bound [Fe-S] cluster to catalytic protein complex BchNB containing a second Fe-S redox center. Interestingly ATP-dependent electron transfer is not restricted to nitrogenase. Instead, Fe-dinitrogenase reductase-like subunits also occur in enzymes such as 2-hydroxyacyl-CoA dehydratase, referred to as "archerases" due to their ability to "activate single electrons" by an ATP-induced change in the redox potential of a [4Fe-4S] center (21).

DPOR from *Rhodobacter capsulatus*, studied using a homologous expression system, consists of BchL and a BchNB complex. Its enzymatic activity requires both ATP and a reducing agent such as dithionite (22, 23), whereas ferredoxin is its physiological electron donor (22). Because *R. capsulatus* DPOR activity declines rapidly after affinity purification, crude cellular extracts were used in these experiments (22).

We have established the first heterologous milligram range production and purification system for *Chlorobium tepidum* DPOR in *Escherichia coli*, allowing the kinetic, spectroscopic, and structural characterization of recombinant wild-type and mutant BchNB and BchL including two [4Fe-4S] clusters and their coordinating cysteine residues.

EXPERIMENTAL PROCEDURES

Production and Purification of C. tepidum DPOR in E. coli—The complete *bchNBL*-operon from *C. tepidum* (strain ATCC 49652) was PCR-amplified using primers CAGGATCCATGATGCCGGTTTCAAG and CAATGCGGCCGCTTACTGCCAGCCACC and cloned into BamHI and NotI sites of pGEX-6P-1 to yield pGEX-*bchNBL*. The *bchL* gene was analogously amplified using primers CAGGATCCATGAGTTTAGTATTGGCC and CAATGCGGCCGCTTACTGCCAGCCACC and cloned into BamHI and NotI sites of pGEX-6P-1 to generate pGEX-*bchL*. The plasmids were transformed into *E. coli* BL21(DE3) Codon Plus RIL to produce the BchNBL complex or only BchL. Cells were cultivated at 17 °C in 500 ml of LB medium with 1 mM Fe(III)-citrate. Protein production was induced by 50 μM isopropyl-β-thiogalactoside at 0.6 OD_{578}. After 16 h of cultivation 1.7 mM dithionite was added and cultivation was continued without agitation for 2 h at 18 °C in an anaerobic chamber (Coy Laboratories, Grass Lake, MI) to allow [Fe-S] cluster formation. All remaining steps were performed under anaerobic conditions at oxygen partial pressure below 1 ppm (Oxygen detector, Coy Laboratories, Grass Lake, MI). Solutions were N_2-saturated prior use. Cells were centrifuged, resuspended in 15 ml of lysis buffer (100 mM HEPES-NaOH (pH 7.5), 10 mM $MgCl_2$, 1 M glycerol, 10 mM dithiothreitol), and disrupted by a single passage through a French press at 1500 p.s.i. into an anaerobic bottle. Following 60 min of centrifugation at 175,000 × *g* at 4 °C, the supernatant was added to 500 μl of glutathione-Sepharose (GE Healthcare) equilibrated with lysis buffer. After washing with 20 ml of phosphate-buffered saline containing 10 mM dithiothreitol (wash buffer) the recombinant fusion protein GST-BchN in complex with BchB or GST-BchL alone were eluted using 2 ml of 50 mM Tris-HCl (pH 8.0) containing 10 mM reduced glutathione. Fractions containing the BchNB complex or GST-BchL were identified by SDS-PAGE.

Purification of the Ternary BchNBL Complex—To obtain a stable ternary DPOR complex, all steps of the affinity purifications were carried out in the presence of 2 or 10 mM BeF_3^-, or 100 or 200 μM AlF_4^- and 5 mM Mg-ADP. Cell-free extracts were incubated with metallofluorides and Mg-ADP 30 min prior to affinity chromatography.

Site-directed Mutagenesis of DPOR Genes and Ribosomal Binding Sites—Up to four nucleotides of the plasmid pGEX-*bchNBL* were exchanged using the QuikChange™ site-directed mutagenesis kit (Stratagene). Oligonucleotides to incrementally optimize the ribosomal binding site of *bchB* (exchanged nucleotides underlined) were: GACGAAAA**G**CAA**A**GA**G**C**A**A-**T**CATGCGTTTAGC; GACGAAAAG**G**AAA**C**AG**T**A**T**TCAT-GCGTTTAGC. Mutations to optimize the ribosomal binding site of *bchL* were: CGATAAACCAATTGAC**G**TC**A**AT**G**AT**T**CCA-TGAGTTTAG; CGATAAACCAATTGACG**A**CA**C**TG**T**TT**T**-CATGAGTTTAG; and CGATAAACCAATTGA**G**GA**A**AC**A**G-T**A**TTCATGAGTTTAG. This expression construct was termed pGEX-*bchNBL**.

Point substitutions in BchN were introduced using the oligonucleotides: C8S, GTTCAAGCGAT**A***GC*CAGATTCTCA-AAG; C21S, CCACAGCTTC**A***GC*GGCCTGGCCTG; C25S, CGGCCTGGCC**AGT**GTCGGCTGGC; C46S, GGTACCCA-CACC**AGC**GCGCACTTTCTCC; C103S, CCTGCTTTCTT-CC**AGT**ACCCCCGAAGTC; C153S, GTGCCCTTC**AGC**CC-CGAAGCTCC; C220S, CTGTCGCGCGTC**AGC**TCGCGC-CTG; and C309S, GGAGGTTGTCGAG**AGC**AGCAGCGCC.

Oligonucleotides for the exchange of codons in *bchB* were: C94S, GTAGCCCCGAGT**AGC**AGCACGGCGC; C94A, CCC-GAGT**GCC**AGCACGGC; C217S, CGTGAGATCGGT**AGC**CA-AGCTGCCGG; C373S, GGAGCTGGTC**AGC**GGCACCCAG; C382S, CGGCACAGC**AGC**CGCAAGCTCG; and C389A, ACGTGCCC**GCC**ATGGTCATTTC.

Oligonucleotides for the exchange of codons in *bchL* were: C38S, GCTCCAGATCGGT**AGC**GACCCGAAGC; C97S, GGA-AGCGGC**AGC**GGCGGCTAC; C131S, CGACGTGGTG**AGC**-GGCGGCTTC; C162S, CCAACCGCCTCT**CC**ATGGCCATTC-AGC; C239S, GCTGGCAGAG**AGC**CTCGCGCC; K10A, GCC-GTTTACGGA**GC**AGGCGGGATC; and ΔL126, TTCTTTTTGATGTGGGCGACGTGGTG.

Protein Concentrations—Concentrations of GST fusion proteins in crude cellular extracts were determined using the GST-detection module (GE Healthcare). The concentration of purified proteins was determined employing the BCA (bicinchoninic acid) protein assay kit (Pierce) and bovine serum albumin as a standard.

N-terminal Amino Acid Sequence Determination—Edman degradation was used to confirm the identity of purified proteins and quantify protein subunits from Western blots.

UV-Visible Light Absorption Spectroscopy—UV-visible light spectra of purified recombinant BchNB complexes and BchL were recorded using a V-550 spectrophotometer (Jasco, Groß Umstadt, Germany) under strict anaerobic conditions.

Iron Determination Method—Protein-bound iron was determined colorimetrically with *o*-phenantroline after acid denaturation of purified BchNB or BchL (24). The iron content of wild-type BchNB and BchL was confirmed by commercial inductively coupled plasma mass spectrometry (ICP-MS) (CURRENTA Bayer-Analytics, Leverkusen, Germany).

Detection of Potential Flavins—Standard detection methods for FMN and FAD cofactors were performed as described elsewhere (25, 26).

Analysis of a Potential Heme Cofactor—The presence of a potential heme cofactor was screened as described elsewhere (27).

Pchlide Preparation—Pchlide was isolated from the *bchL*-deficient *R. capsulatus* strain ZY5 as described earlier (23).

Pchlide Reduction Assay—DPOR activity was measured in 250-μl assays in 100 mM Hepes-NaOH (pH 7.5), 2 mM ATP, 5 mM $MgCl_2$, 20 μM Pchlide, and 10 mM dithiothreitol as electron donor and an ATP regenerating system (20 mM creatine phosphate and 20 units of creatine phosphokinase/assay). This standard DPOR assay was supplemented with 30–100 μl of cell-free *E. coli* extract containing overproduced GST-BchN, BchB, and BchL. In DPOR reconstitution assays, 20 μg of BchNB complex and 20–60 μg of GST-BchL fusion protein were added. After 30–70 min at 35 °C under strict anaerobic conditions in the dark, reactions were stopped by 1 ml of acetone. Pchlide and Chlide in supernatants obtained by centrifuging for 10 min at 12,000 × *g* were spectrophotometrically quantified using extinction coefficient $\epsilon_{626} = 30.4\ mM^{-1}\ cm^{-1}$ for Pchlide (23) and $\epsilon_{665} = 74.9\ mM^{-1}\ cm^{-1}$ for Chlide (28). To investigate the ability of ferredoxin to function as elctron donor, the reconstitution assay was supplemented with a ferredoxin regenerating system (13 mM glucose 6-phosphate, 1.1 unit of glucose-6-phosphate dehydrogenase from Torula yeast (Sigma), 1.64 mM $NADP^+$, and 0.025 units of ferredoxin-$NADP^+$ oxidoreductase from spinach (Sigma)). The assay was also supplemented with commercially available ferredoxins from *Clostridium*, *Porphyra*, or spinach (Sigma) or with recombinantly produced ferredoxin from *Synechococcus* (29) at a concentration of 25 μg/ml, respectively.

Activation Energy of DPOR Catalysis—To determine the activation energy of ATP-driven DPOR catalysis, the standard assay was repeated between 291 and 319 K. The initial rate of Chlide formation was used to calculate the rate constant at each temperature and the activation energy was determined by the Arrhenius equation,

$$\ln k = (-E_{act}/R \cdot T) + c \qquad \text{(Eq. 1)}$$

where k is the rate constant, E_{act} the activation energy, R the gas constant (8.314 kJ mol^{-1} K^{-1}), T the temperature (K), and c a reaction constant.

CN^- Inhibition of DPOR—To analyze the inhibitory effect of CN^- on DPOR catalysis, standard DPOR assays were carried out in the presence of 0–60 mM sodium cyanide.

Molecular Mass Determination—Analytical gel permeation chromatography was performed using a Superdex 200 HR 10/30 column (GE Healthcare), equilibrated with wash buffer containing 100 mM NaCl. The column was calibrated with protein standards (Molecular Weight Marker Kit MW-GF 1000, Sigma) at a flow rate of 0.5 ml min^{-1}. A 15-μl sample of purified BchNB or BchL (~45 μg) was run under identical conditions (30).

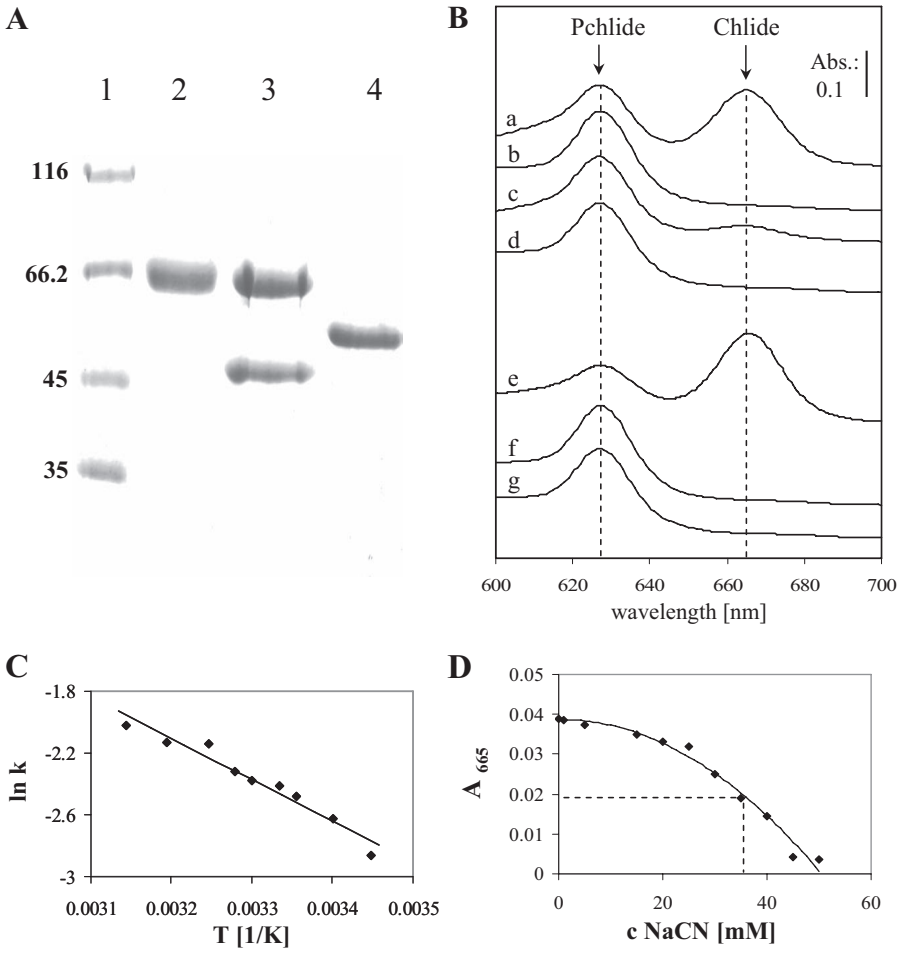

FIGURE 3. **Purification of recombinant *C. tepidum* DPOR subunits, catalytic activity, activation energy, and CN^- inhibition assays.** *A*, SDS-PAGE analyses of purified, recombinant BchNB complex and BchL. *Lane 1*, molecular size marker, masses as indicated (×1000); *lane 2*, purified GST-BchN complexed with BchB, cell extracts from *E. coli* BL21(DE3) Codon Plus RIL containing pGEX-*bchNBL** after isopropyl β-D-thiogalactopyranoside induction, affinity chromatography on glutathione-Sepharose, extensive washing, and glutathione elution; *lane 3*, BchN and BchB were recovered from glutathione-Sepharose after proteolytic cleavage; *lane 4*, *E. coli* extracts from cells containing pGEX-*bchL* after isopropyl β-D-thiogalactopyranoside induction, affinity chromatography on glutathione-Sepharose, extensive washing, and glutathione elution. *B*, absorption spectra of standard DPOR assays using *E. coli* cell extracts or reconstitution assays after 20 min at 35 °C and acetone extraction. *Trace a*, standard DPOR assay containing 30 μl of *E. coli* extract; *trace b*, assay mixture without dithionite; *trace c*, assay mixture without ATP; *trace d*, control reaction without cell extract; *trace e*, reconstitution assay using 20 μg of purified $(BchNB)_2$ and 20 μg of purified $BchL_2$; *trace f*, control reaction using 20 μg of $(BchNB)_2$ but no $BchL_2$; *trace g*, control reaction using 20 μg of $BchL_2$ but no $(BchNB)_2$. *C*, determination of the activation energy of DPOR catalysis. In an Arrhenius plot the logarithm of activity (ln *k*, where *k* is the initial rate of Chlide formation in the standard DPOR assay) is plotted *versus* the reciprocal of the absolute temperature in K. *D*, cyanide inhibition of DPOR. The activity of standard DPOR assays (15 min at 35 °C) in the presence of 0–60 NaCN is plotted against the concentration of NaCN. 50% inhibition of DPOR is achieved at 36 mM NaCN.

Molybdenum Cofactor Analysis—To identify a possible molybdenum cofactor coordinated by BchNB, the nit-1 reconstitution assay supplemented with 4 μg of BchNB was used (31). 1.2 mg of BchNB were used to detect the stable oxidation product FormA of the cofactor (32). Subsequent product dephosphorylation, sample preparation, and HPLC analysis were performed as published (33).

DPOR Production by Strains of E. coli Defective in Molybdenum Uptake—DPOR was produced by transforming *pGEX-bchNBL** into *E. coli* RK-5207, a strain unable to import molybdenum from the medium (34, 35). To overcome the phenotype of the RK-5207 mutant, DPOR was concurrently produced in the presence of 1 and 10 mM Na_2MoO_4 in LB medium. DPOR activity was tested in cell-free extracts.

Molybdenum and Vanadium Determination by ICP-MS—To rule out the involvement of molybdenum or vanadium in DPOR catalysis ICP-MS was performed (36, 37). Samples containing 5 μg of purified protein were applied to the ICP-MS.

RESULTS AND DISCUSSION

C. tepidum DPOR Produced in E. coli Is Enzymatically Active—The complete *bchNBL* operon of the thermophilic green sulfur bacterium *C. tepidum* was cloned into a standard *E. coli* expression vector, producing the DPOR subunit BchN as an N-terminal glutathione *S*-transferase fusion protein (pGEX-*bchNBL*). However, amounts of recombinant proteins and DPOR activity were found to be low. Replacing the *C. tepidum*-type ribosomal binding site upstream of *bchB* (CCAACGAACCAA) and *bchL* (CCTCTATCATAC) with an *E. coli* type ribosomal binding site (GGAAACAGTATT) resulted in an expression vector (pGEX-*bchNBL**) that allows significant amounts of BchB and BchL to be produced (data not shown). Concomitantly, the DPOR activity of *E. coli* cell extracts increases from 0.29 to 3.15 nmol min^{-1} mg^{-1} (standard DPOR assay, 35 °C) (Fig. 3*B*, *traces a–d*), a significant improvement in specific activity compared with ~40 pmol min^{-1} mg^{-1} for DPOR from *R. capsulatus* cell-free extracts (23). Despite distinct homology to nitrogenase, DPOR activity does not require further enzymes, such as molybdenum cofactor biosynthesizing or incorporating proteins, known to be essential to nitrogenase-producing organisms. Orthologues of genes encoding these proteins are not found in the genome of the *E. coli* production host.

Purification of the Heterotetrameric BchNB Complex—DPOR was maintained under strict anaerobic conditions throughout, including during cell harvesting, cell disruption, protein purification, and activity assays. BchN was purified from *E. coli* pGEX-*bchNBL** extracts. GST-BchN fusion protein was coupled to glutathione-Sepharose, washed extensively, and either eluted intact with 10 mM glutathione (Fig. 3*A*, *lane 2*)

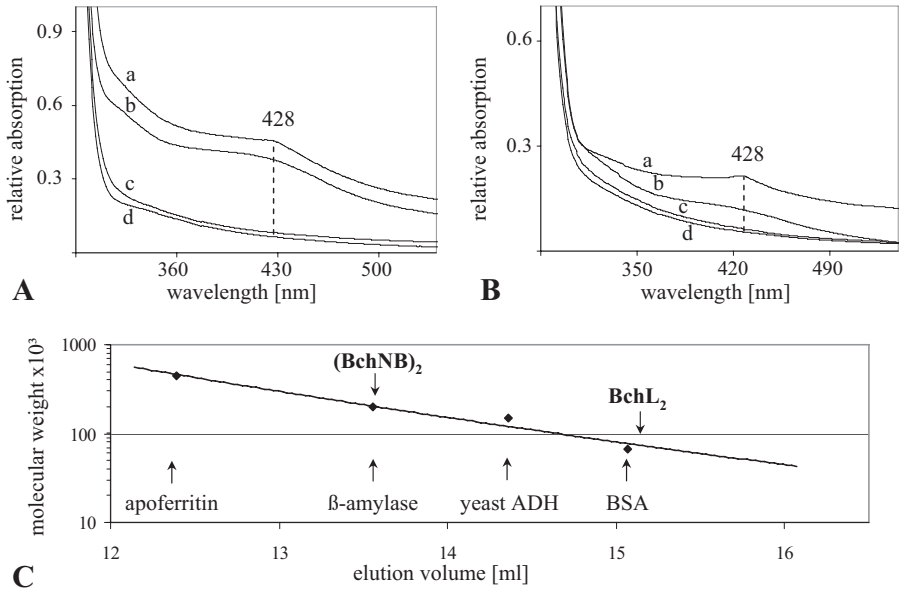

FIGURE 4. **UV-visible absorption spectroscopy and relative molecular masses of BchNB and BchL.** UV-visible light absorption spectra of $(BchNB)_2$ (*A*) and $BchL_2$ (*B*). Spectra were recorded under anaerobic conditions with protein concentrations of 3.7 mg/ml $(BchNB)_2$ and 1.6 mg/ml $BchL_2$. *Spectra a*, protein samples purified anaerobically; *spectra b*, protein samples reduced with sodium dithionite (2 mM, 1 h); *spectra c*, samples exposed to oxygen for 15 h; *spectra d*, samples after EDTA treatment (10 mM, 2 h). *C*, analytical gel filtration of BchNB and BchL. 45 μg of affinity purified proteins after protease cleavage were analyzed on a Superdex 200 HR 10/30 column under anaerobic conditions using a flow rate of 0.5 ml/min and monitoring the absorption at 280 and 428 nm. Protein standards were bovine serum albumin (*BSA*) (M_r = 66,000), yeast alcohol dehydrogenase (M_r = 150,000), β-amylase (M_r = 200,000), and apoferritin (M_r = 443,000). The inferred mass of BchNB is $M_r = 210{,}000 \pm 10{,}000$ indicating a $(BchNB)_2$ tetramer, whereas that of BchL is $M_r = 60{,}000 \pm 5{,}000$ indicating a BchL dimer ($BchL_2$).

or liberated from bound GST by PreScission protease treatment (Fig. 3*A*, *lane 3*). SDS-PAGE analyses confirm the masses of GST-BchN (M_r = 74,000) or BchN (M_r = 47,000) and reveal stoichiometric amounts of a second protein (M_r = 59,000) (Fig. 3*A*, *lanes 2* and *3*). By N-terminal amino acid sequencing BchB was identified in equimolar amounts. The molecular mass of the BchNB complex was estimated to be M_r = 210,000 by gel filtration (Fig. 4*C*) implying a stoichiometry of 2BchN (46,643 Da each) and 2BchB (58,968 Da each). Henceforth the complex is therefore denoted $(BchNB)_2$. Overall, we purified 2 mg of pure $(BchNB)_2$ complex per liter of medium.

Purification of the Homodimeric BchL Complex—To allow reconstitution of DPOR, the subunit BchL was separately purified from *E. coli* extracts. The GST-BchL fusion protein was purified by affinity chromatography and eluted as GST fusion protein with 10 mM glutathione buffer or cleaved off GST by PreScission protease. SDS-PAGE analysis indicates a single protein of M_r = 57,000 for GST-BchL (Fig. 3*A*, *lane 4*) or M_r = 30,000 for BchL. Analytical gel filtration revealed a relative molecular mass of about 60,000 (Fig. 4*C*) for BchL indicating that purified BchL from *C. tepidum* is homodimeric, henceforth denoted $BchL_2$. Overall, 1.5 mg of pure $BchL_2$ were recovered from 5 liters of *E. coli* culture.

Reconstitution of DPOR Activity—To reconstitute DPOR activity *in vitro*, 20 μg (0.1 nmol) of $(BchNB)_2$ and 20–60 μg (0.7–2 nmol) of BchL were assayed using 20 μM Pchlide in the presence of 10 mM dithionite as reductant, 2 mM ATP, and an ATP regenerating system. After 20 min incubation under anaerobic conditions at 35 °C, the reactions were stopped by adding 80% (v/v) acetone. Photometric analysis indicated that the reconstituted *C. tepidum* enzyme efficiently converts Pchlide (absorbance maximum 626 nm) into Chlide (absorbance maximum 665 nm; Fig. 3*B*, *trace e*). Chlide production was not detected if BchNB (*trace f*), BchL (*trace g*), dithionite, or the ATP regenerating system were omitted, or when the assay was performed under aerobic conditions (data not shown).

Kinetic Properties of DPOR Catalysis—To establish the K_m values for *C. tepidum* DPOR we determined the initial velocity of Chlide formation over a broad range of Pchlide, ATP, and dithionite concentrations using the outlined DPOR assay and saturating concentrations for the residual substrates. For Pchlide, ATP, and the artificial co-substrate dithionite, Chlide formation followed Michaelis-Menten kinetics. The apparent K_m for Pchlide was found to be 6.1 μM, slightly lower than the 10.6 μM measured for DPOR from *R. capsulatus* (22). The K_m of *C. tepidum* DPOR for ATP was 13.5 μM, and 52.7 μM for dithionite (supplemental data Fig. 1).

Ferredoxin-dependent C. tepidum DPOR Activity—To identify the true electron donor of DPOR, we replaced dithionite with [2Fe-2S]-ferredoxins from *Synechococcus sp. PCC 7002*, *Porphyra umbilicalis*, *Spinacia oleracea*, and with a [4Fe-4S]-ferredoxin from *Clostridium pasteurianum* in standard DPOR assays, supplemented with a ferredoxin-regenerating system: glucose 6-phosphate, glucose-6-phosphate dehydrogenase from Torula yeast (Sigma), $NADP^+$, and ferredoxin-$NADP^+$ oxidoreductase from spinach (Sigma). Only the ferredoxin from *Synechococcus* achieved 10% of the dithionite-supported DPOR activity. As other ferredoxins fail to sustain DPOR activity, we propose that a plant-type [2Fe-2S]-ferredoxin might be the electron donor for *C. tepidum* DPOR *in vivo*, corroborating the observation that [2Fe-2S]-ferredoxin from maize is an electron donor for DPOR from *R. capsulatus* (22).

Thermodynamic Properties of Pchlide Reduction by C. tepidum DPOR—Initial rates of Chlide formation were used to calculate rate constants at various temperatures. An Arrhenius plot of ln *k versus* 1/T indicates an activation energy for DPOR electron transfer of 22.2 kJ mol^{-1} (Fig. 3*C*), only slightly higher than the 18.8 kJ mol^{-1} reported for light-driven Pchlide reduction by LPOR (6) but dramatically lower than the 90–97 kJ mol^{-1} required for the electron transfer from the Fe-protein to the MoFe-protein of nitrogenase (38, 39). The nitrogenase reaction is exergonic by ~64 kJ mol^{-1} (40). Overall, nitrogenase requires 16 ATP molecules to overcome the kinetic barrier for the reduction of nitrogen (40). Pchlide reduction is similarly

TABLE 1

Enzymatic activities, iron, and sulfur content of mutant DPOR enzymes

The specific enzymatic activity of the wild-type DPOR (3.15 nmol min^{-1} mg^{-1}) was set as 100%. The iron and sulfur contents per mol of purified wild-type $(BchNB)_2$ and $BchL_2$ were set as 100%. DPOR protein variants *bchN* C46S, *bchN* C103S, *bchL* C97S, *bchL* C131S, *bchL* K10A, and *bchL* ΔL126 were additionally tested with 260 μg of $(BchNB)_2$ and 200 μg of $BchL_2$ per assay with an increased incubation time for up to 4 hs. Obtained activities were below to the detection limit of the assay at 15.75 nmol min^{-1} mg^{-1}.

mutation	[Fe-S] coordinating Cys	residues DPOR	conserved in nitrogenase	enzymatic turnover [%]	iron content [%]	sulfur content [%]	
bchN C8S		-	-	100	100	100	
bchN C21S	+	+	+	2	23	25	
bchN C25S		+	-	100	100	100	
bchN C46S	+	+	+	< 0.5	40	13	
bchN C103S	+	+	+	< 0.5	44	42	
bchN C153S		+	-	100	100	100	
bchN C220S		-	-	100	100	100	
bchN C309S		-	-	100	100	100	$(BchNB)_2$
bchB C94S	+	+	+	20	85	43	
bchB C94A	+	+	+	5	25	21	
bchB C217S		-	-	100	100	100	
bchB C373S		-	-	100	100	85	
bchB C382S		-	-	100	83	67	
bchB C389S		+	+	70	100	85	
bchL C38S		+	+	100	100	75	
bchL C97S	+	+	+	< 0.5	25	15	
bchL C131S	+	+	+	< 0.5	2	15	
bchL C162S		+	+	100	100	66	$BchL_2$
bchL C239S		C, S or A	C, S or A	80	55	52	
bchL K10A		+	+	< 0.5	100	100	
bchL L126		+	+	< 0.5	100	100	

exergonic with a ΔH ~40 kJ mol^{-1} (5). As the kinetic barrier to DPOR catalysis is only a quarter that of nitrogenase, at least 4 molecules of ATP would be required to transfer two electrons during the reduction of Pchlide. The even number of ATP molecules would match the dimeric nature of $BchL_2$, whereas electron transfer presumably occurs via the inter subunit [Fe-S] cluster as in nitrogenase.

CN^- Resistance of DPOR—To establish whether CN^- also uncouples ATP hydrolysis from electron transport in DPOR as observed in nitrogenase (41), the effect of CN^- on DPOR catalysis was analyzed with the standard DPOR assay. Plotting the DPOR activity (Chlide formation) against CN^- concentration (Fig. 3*D*) indicates that 36 mM NaCN is required to reduce DPOR activity by half, significantly higher than the 5 mM NaCN for *A. vinelandii* nitrogenase (Mo-nitrogenase) (42). The metal centers of $(BchNB)_2$ are thus clearly not as sensitive with respect to CN^- as those of nitrogenase, indicating distinct differences in the metal centers of DPOR and nitrogenase.

Cysteine Residues Cys^{97} and Cys^{131} of BchL Coordinate an Intersubunit Iron-Sulfur Cluster—Purified, GST-tagged $BchL_2$ is brownish in color. A UV-visible light absorption spectrum recorded under strict anaerobic conditions reveals an absorption peak at 428 nm typical for a [4Fe-4S] cluster (Fig. 4*B*, *spectrum a*). The absorption in the range of 390–428 nm bleaches after addition of the reductant dithionite (2 mM, 1 h) (Fig. 4*B*, *spectrum b*), whereas oxidation by oxygen exposure for 15 h (Fig. 4*B*, *spectrum c*) as well as EDTA treatment (10 mM, 2 h) completely abolishes the absorption in this area of the spectrum. This observation is in accordance to UV-visible spectra obtained for proteins containing iron-sulfur redox clusters (43–45). By applying an extinction coefficient for [4Fe-4S] clusters of $\epsilon_{410} = 15$ mM^{-1} cm^{-1} (44, 46) we calculated 0.9 mol of [4Fe-4S] cluster per mol of $BchL_2$. This ratio was confirmed by ICP-MS quantification revealing 3.62 mol of iron/mol of $BchL_2$. Amino acid sequence alignments of BchL proteins reveal five conserved cysteines. Each cysteine was individually substituted by serine to identify potential iron-sulfur cluster ligands. Only variants C97S and C131S cause a significant loss in DPOR activity to <0.5%, whereas C38S and C162S retain 100% and C239S 80% of wild-type activity. Correspondingly, the iron and sulfur content of BchL variants C97S and C131S only were reduced (Table 1). These cysteines thus presumably coordinate the inter-subunit [4Fe-4S] cluster, analogous to Cys^{97} and Cys^{132} in $NifH_2$. These results are in good agreement with a recent study for *R. capsulatus* DPOR, where an EPR signal for a [4Fe4S] cluster was obtained (47).

Residues Lys^{10} and Leu^{126} of BchL Are Essential to Catalysis—In nitrogenase, binding of $NifH_2$ to $(NifDK)_2$ is dependent upon ATP-induced conformational changes. Subsequent ATP hydrolysis induces further conformational rearrangements that decrease the redox potential of the $NifH_2$ [4Fe-4S] cluster, transferring a single electron to $(NifDK)_2$, followed by the dis-

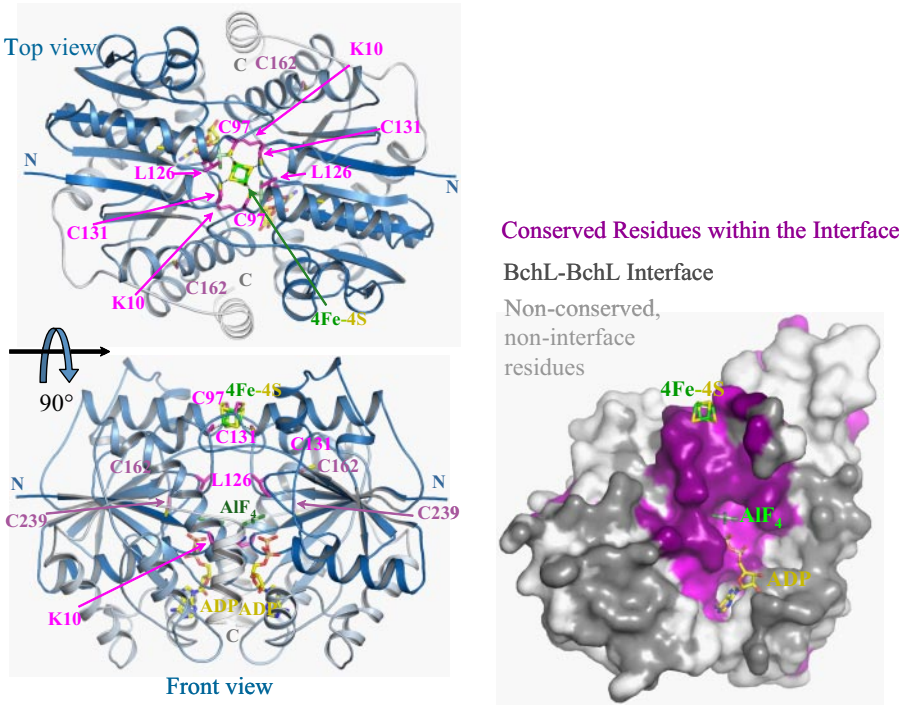

FIGURE 5. **Ribbon diagram of dimeric BchL.** $NifH_2$ in the ADP-AlF_4^- bound state (PDB code 1M34) was used to generate the model of $BchL_2$. Dimeric BchL is shown in two mutually perpendicular orientations. The [4Fe-4S] cluster is coordinated by cysteines Cys^{97} and Cys^{131} of each subunit at the interface of the dimer. The positions of Lys^{10} (P-loop), Leu^{126} (switch II), and the ATP binding site are shown.

sociation of $NifH_2$ from $(NifDK)_2$. Two sequence motifs are crucial to ATP-binding and subsequent signal transmission. The "switch II" motif DVLGDVVCGG conformationally relays ATP binding to the [4Fe-4S] cluster *inter alia* by repositioning cluster ligand Cys^{132}. Deleting Leu^{127} of the switch II motif traps $NifH_2$ in a conformation preventing hydrolysis of ATP thus inactivating nitrogenase (48). This "trapped" $NifH_2$ variant forms a stable ternary complex with $(NifDK)_2$ allowing simple co-purification. The N-terminal P-loop region G*XXXX*GK(S/T) coordinates the γ-phosphate of ATP primarily by Lys^{15} (*A. vinelandii* numbering). Replacing Lys^{15} by glutamine completely inactivates nitrogenase despite ATP binding being unaffected.

Lys^{15} and Leu^{127} of NifH correspond to Lys^{10} and Leu^{126} of BchL, conserved in all BchL protein sequences. Mutating *bchL* to produce the variants K10A and L126Δ (Leu^{126} deleted) in the plasmid pGEX*bchNBL** results in a specific activity <0.5% of wild-type DPOR. Lys^{10} and Leu^{126} are thus essential for DPOR catalysis indicating that ATP hydrolysis and electron transfer in DPOR may be analogous to nitrogenase. Attempts to purify a ternary BchNBL complex using either BchL variant L126Δ or Mg-ADP in combination with metallofluorides (AlF_4^- and BeF_3^-), in analogy to nitrogenase, were not successful, indicating differences in the transient interaction of $BchL_2$ with $(BchNB)_2$ to nitrogenase (18).

Three-dimensional Structural Model of BchL—The amino acid sequence of BchL of DPOR shares a sequence identity of 33% with that of NifH of nitrogenase, allowing for three insertions/deletions involving nine residues distinguish BchL and NifH. Based on the structure of ATP-bound $NifH_2$ in complex with $(NifDK)_2$ (Protein data bank code 1M34) (49), we produced a structural model of BchL (Fig. 5) using SwissModel (50) and Bragi (51). Conserved and conservatively replaced residues of BchL and NifH are located in the immediate vicinity of the [4Fe-4S] cluster, the BchL-BchL interface, the ATP-binding pocket, and the protein core of each subunit. Conversely, essentially no conservation of amino acids is observed on the surface of the BchL-monomer outside of the BchL-BchL interface. This is also true for the surface involved in binding $(BchNB)_2$, indicating that the subunits of both DPOR and nitrogenase have evolved to optimize recognition within each complex but diverged to prevent cross-interaction between related subunits of alternate complexes. The conservation of residues at the dimer interface, the iron-sulfur cluster, and the ATP-binding site, supports the idea of a bridging [4Fe-4S] cluster in $BchL_2$ (see above) coordinated by cysteine residues Cys^{97} and Cys^{131} and that $BchL_2$ utilizes a related ATP-controlled gating mechanism to transfer electrons to $(BchNB)_2$. The structural $BchL_2$ model, furthermore, places residues Cys^{38}, Cys^{162}, and Cys^{239} within the hydrophobic core of each subunit, corroborating the interpretation that these cysteines are not involved in iron-sulfur cluster coordination. Substituting Cys^{239} by serine presumably destabilizes the protein as a whole, explaining the observed partial loss of DPOR activity of the mutant C239S.

DPOR Catalysis Is Independent of a Molybdenum Cofactor—The presumed evolutionary relationship of DPOR to nitrogenase is supported by the similarity of the amino acid sequences of BchN, BchB, and BchL to those of NifD, NifK, and NifH as well as by the identical oligomeric state of $(BchNB)_2$ and $(NifDK)_2$, and of $BchL_2$ and $NifH_2$. This raises the question regarding conserved metal centers.

To identify a potential molybdopterin cofactor, $(BchNB)_2$ was analyzed by the *nit-1* complementation assay. The mutant *nit-1* of *Neurospora crassa* is deficient in molybdenum cofactor biosynthesis, producing a stable apo-form of nitrite reductase. In cell-free extracts of this mutant, nitrite reductase activity can be restored by adding molybdenum cofactor (31). Purified $(BchNB)_2$ is not able to complement this mutant. HPLC analyses failed to detect the stable oxidation product FormA-dephospho of molybdopterin in purified $(BchNB)_2$. Next we produced DPOR in *E. coli* strain RK-5207 deficient in molybdenum uptake (52). Mo-protein synthesis in RK-5207 may be rescued by adding MoO_4^{2-} to the growth medium (34, 35). The amount of active DPOR produced by *E. coli* RK-5207 is similar to that of *E. coli* strain DH10B without addition of MoO_4^{2-}. Instead 1 mM MoO_4^{2-} in

the growth medium decreases DPOR activity by ~70%. Clearly, production of active DPOR in *E. coli* does not require molybdenum.

Correspondingly, ICP-MS analyses of purified $(BchNB)_2$ indicated molybdenum and vanadium concentrations no higher than those of the negative controls. $(BchNB)_2$, in contrast to the MoFe-protein of nitrogenase, thus does not bind nor require a molybdenum cofactor.

$(BchNB)_2$ Contains Two Iron-Sulfur Clusters—Under anaerobic conditions, concentrated $(BchNB)_2$ solutions are brownish in color. UV-visible light absorption spectra correspondingly revealed an absorption maximum at 428 nm typical for [4Fe-4S] clusters (Fig. 4*A*, *spectrum a*). Reduction with dithionite (2 mM, 1 h) decreases the absorption maximum (Fig. 4*A*, *spectrum b*), whereas oxygen exposure for 15 h as well as EDTA treatment (10 mM, 2 h) completely bleaches the absorption in the range of 390–428 nm as described elsewhere (43–45). We calculated 1.8 mol of [4Fe-4S] cluster/mol of $(BchNB)_2$ when using a standard extinction coefficient for [4Fe-4S] clusters of $\epsilon_{410} = 15\ mM^{-1}\ cm^{-1}$ (44, 46). ICP-MS analyses result in 7.33 mol of iron/mol of $(BchNB)_2$ indicating the presence of two [4Fe-4S] clusters per $(BchNB)_2$ tetramer. Standard methods failed to detect additional heme and flavin cofactors.

Cysteines Cys^{21}, Cys^{46}, Cys^{103} of BchN and Cys^{94} of BchB Participate in Iron-Sulfur Cluster Coordination—All cysteines in BchN (eight) and BchB (five) were individually replaced by serines by site-directed mutagenesis to identify [Fe-S] cluster ligands. BchN variants C21S, C46S, and C103S show <0.5% residual activity and are essentially inactive (Table 1). BchB variants C94S and C389S, by contrast retain 20 and 70% of the wild-type activity. Interestingly activity of C94A is reduced to 5% indicating that Ser^{94} may functionally substitute cysteine as a [Fe-S] ligand (53). Correspondingly, the iron and sulfur content of $(BchNB)_2$ complexes bearing substitutions $C21S_{BchN}$, $C46S_{BchN}$, $C103S_{BchN}$, and $C94A_{BchB}$ amount to only 0.8–1.8 mol of iron and 0.5–1.5 mol of S/mol of $(BchNB)_2$ (Table 1), whereas those bearing substitutions $C8S_{BchN}$, $C25S_{BchN}$, $C46S_{BchN}$, $C153S_{BchN}$, $C220S_{BchN}$ $C309S_{BchN}$ and $C217S_{BchB}$, $C373S_{BchB}$, $C382S_{BchB}$, $C389S_{BchB}$ are comparable with that of the wild-type enzyme. Combining the mutagenesis data with UV-visible spectroscopy, we infer that tetrameric $(BchNB)_2$ contains two inter-subunit [4Fe-4S] clusters each coordinated by Cys^{21}, Cys^{46}, and Cys^{103} of BchN and Cys^{94} of BchB.

Proposed Enzymatic Mechanism for DPOR—Summarizing the above inferences, we propose that one of the two "plant type" [2Fe-2S]-ferredoxins in the genome of *C. tepidum* might be the natural electron donor of DPOR. The P-loop region (incorporating Lys^{10}) and the switch II region (Leu^{126}) are crucial for ATP-binding and dynamic positioning. We, furthermore, expect two molecules of ATP to bind per BchL dimer. Because the activation energy (22.2 kJ mol^{-1}) for Pchlide reduction is a fourth that of nitrogenase, we propose that at least four molecules of ATP are required to overcome the kinetic barrier to the two-electron reduction of Pchlide. This scenario is in good agreement with the dimeric state of $BchL_2$, presumably bridged by an intersubunit [4Fe-4S] cluster. The cluster would transfer a single electron to a second intersubunit [4Fe-4S] cluster coordinated by both BchN and BchB within the $(BchNB)_2$ complex. This second cluster then transfers the electron to the substrate, resulting in a reduced Pchlide radical. Consumption of another two ATP molecules by $BchL_2$ would then allow a second electron to follow the first, resulting in fully reduced Chlide.

Acknowledgments—We thank Carl E. Bauer for providing R. capsulatus strain ZY5. We are indebted to Ralf R. Mendel for E. coli strain RK-5207 and helpful discussions, Rita Getzlaff for N-terminal protein sequencing, and Gabriele Günther for continuous support during mutagenesis.

REFERENCES

1. Fujita, Y. (1996) *Plant Cell Physiol.* **37,** 411–421
2. Schoefs, B. (2001) *Photosynth. Res.* **70,** 257–271
3. Apel, K. (2001) in *Regulation of Photosynthesis* (Aro, E.-M., and Anderson, B., eds) pp. 235–252, Kluwer Akademic Publishers, Dordrecht
4. Belyaeva, O. B., Griffiths, W. T., Kovalev, J. V., Timofeev, K. N., and Litvin, F. F. (2001) *Biochemistry* (*Mosc.*) **66,** 173–177
5. Heyes, D. J., Hunter, C. N., van Stokkum, I. H., van Grondelle, R., and Groot, M. L. (2003) *Nat. Struct. Biol.* **10,** 491–492
6. Heyes, D. J., Ruban, A. V., Wilks, H. M., and Hunter, C. N. (2002) *Proc. Natl. Acad. Sci. U. S. A.* **99,** 11145–11150
7. Rüdiger, W. (2003) in *Porphyrin Handbook, Chlorophylls and Bilins: Biosynthesis, Synthesis, and Degradation* (Kadish, K. M., Smith, K. M., and Guilard, R., eds) Vol. 13, pp. 71–108, Academic Press, New York
8. Masuda, T., and Takamiya, K. (2004) *Photosynth. Res.* **81,** 1–29
9. Xiong, J., Inoue, K., and Bauer, C. E. (1998) *Proc. Natl. Acad. Sci. U. S. A.* **95,** 14851–14856
10. Suzuki, J. Y., Bollivar, D. W., and Bauer, C. E. (1997) *Annu. Rev. Genet.* **31,** 61–89
11. Bollivar, D. W., Suzuki, J. Y., Beatty, J. T., Dobrowolski, J. M., and Bauer, C. E. (1994) *J. Mol. Biol.* **237,** 622–640
12. Burke, D. H., Alberti, M., and Hearst, J. E. (1993) *J. Bacteriol.* **175,** 2414–2422
13. Burke, D. H., Hearst, J. E., and Sidow, A. (1993) *Proc. Natl. Acad. Sci. U. S. A.* **90,** 7134–7138
14. Fujita, Y., Matsumoto, H., Takahashi, Y., and Matsubara, H. (1993) *Plant Cell Physiol.* **34,** 305–314
15. Rees, D. C., Akif Tezcan, F., Haynes, C. A., Walton, M. Y., Andrade, S., Einsle, O., and Howard, J. B. (2005) *Philos. Transact. A Math. Phys. Eng. Sci.* **363,** 971–984, 1035–1040
16. Peters, J. W., Fisher, K., and Dean, D. R. (1995) *Annu. Rev. Microbiol.* **49,** 335–366
17. Dean, D. R., Bolin, J. T., and Zheng, L. (1993) *J. Bacteriol.* **175,** 6737–6744
18. Igarashi, R. Y., and Seefeldt, L. C. (2003) *Crit. Rev. Biochem. Mol. Biol.* **38,** 351–384
19. Lanzilotta, W. N., Fisher, K., and Seefeldt, L. C. (1997) *J. Biol. Chem.* **272,** 4157–4165
20. Ryle, M. J., Lanzilotta, W. N., and Seefeldt, L. C. (1996) *Biochemistry* **35,** 9424–9434
21. Kim, J., Hetzel, M., Boiangiu, C. D., and Buckel, W. (2004) *FEMS Microbiol. Rev.* **28,** 455–468
22. Nomata, J., Swem, L. R., Bauer, C. E., and Fujita, Y. (2005) *Biochim. Biophys. Acta* **1708,** 229–237
23. Fujita, Y., and Bauer, C. E. (2000) *J. Biol. Chem.* **275,** 23583–23588
24. Lovenberg, W., Buchanan, B. B., and Rabinowitz, J. C. (1963) *J. Biol. Chem.* **238,** 3899–3913
25. Yu, S. W., Kim, Y. R., and Kang, S. O. (1999) *Biochem. J.* **341,** 755–763
26. Heinemann, I. U., Diekmann, N., Masoumi, A., Koch, M., Messerschmidt, A., Jahn, M., and Jahn, D. (2007) *Biochem. J.* **402,** 575–580
27. Sun, W. (2005) *J. Chem. Sci.* **117,** 317–322
28. McFeeters, R. F., Chichester, C. O., and Whitaker, J. R. (1971) *Plant*

Physiol. **47,** 609–618
29. Dammeyer, T., and Frankenberg-Dinkel, N. (2006) *J. Biol. Chem.* **281,** 27081–27089
30. Layer, G., Verfurth, K., Mahlitz, E., and Jahn, D. (2002) *J. Biol. Chem.* **277,** 34136–34142
31. Havemeyer, A., Bittner, F., Wollers, S., Mendel, R., Kunze, T., and Clement, B. (2006) *J. Biol. Chem.* **281,** 34796–34802
32. Rajagopalan, K. V., Johnson, J. L., and Hainline, B. E. (1982) *Fed. Proc.* **41,** 2608–2612
33. Schwarz, G., Boxer, D. H., and Mendel, R. R. (1997) *J. Biol. Chem.* **272,** 26811–26814
34. Stewart, V., and MacGregor, C. H. (1982) *J. Bacteriol.* **151,** 788–799
35. Campbell, A. M., del Campillo-Campbell, A., and Villaret, D. B. (1985) *Proc. Natl. Acad. Sci. U. S. A.* **82,** 227–231
36. Llamas, A., Otte, T., Multhaup, G., Mendel, R. R., and Schwarz, G. (2006) *J. Biol. Chem.* **281,** 18343–18350
37. Simons, A., Ruppert, T., Schmidt, C., Schlicksupp, A., Pipkorn, R., Reed, J., Masters, C. L., White, A. R., Cappai, R., Beyreuther, K., Bayer, T. A., and Multhaup, G. (2002) *Biochemistry* **41,** 9310–9320
38. Mensink, R. E., and Haaker, H. (1992) *Eur. J. Biochem.* **208,** 295–299
39. Lanzilotta, W. N., Parker, V. D., and Seefeldt, L. C. (1998) *Biochemistry* **37,** 399–407
40. Kurnikov, I. V., Charnley, A. K., and Beratan, D. N. (2001) *J. Phys. Chem.* **105,** 5359–5367
41. Li, J., Burgess, B. K., and Corbin, J. L. (1982) *Biochemistry* **21,** 4393–4402
42. Fisher, K., Dilworth, M. J., and Newton, W. E. (2006) *Biochemistry* **45,** 4190–4198
43. Anderson, G. L., and Howard, J. B. (1984) *Biochemistry* **23,** 2118–2122
44. Hanzelmann, P., Hernandez, H. L., Menzel, C., Garcia-Serres, R., Huynh, B. H., Johnson, M. K., Mendel, R. R., and Schindelin, H. (2004) *J. Biol. Chem.* **279,** 34721–34732
45. Agar, J. N., Krebs, C., Frazzon, J., Huynh, B. H., Dean, D. R., and Johnson, M. K. (2000) *Biochemistry* **39,** 7856–7862
46. Shen, G., Balasubramanian, R., Wang, T., Wu, Y., Hoffart, L. M., Krebs, C., Bryant, D. A., and Golbeck, J. H. (2007) *J. Biol. Chem.* **282,** 31909–31919
47. Nomata, J., Kitashima, M., Inoue, K., and Fujita, Y. (2006) *FEBS Lett.* **580,** 6151–6154
48. Ryle, M. J., and Seefeldt, L. C. (1996) *Biochemistry* **35,** 4766–4775
49. Schmid, B., Einsle, O., Chiu, H. J., Willing, A., Yoshida, M., Howard, J. B., and Rees, D. C. (2002) *Biochemistry* **41,** 15557–15565
50. Schwede, T., Kopp, J., Guex, N., and Peitsch, M. C. (2003) *Nucleic Acids Res.* **31,** 3381–3385
51. Reichelt, J., Dieterich, G., Kvesic, M., Schomburg, D., and Heinz, D. W. (2005) *Bioinformatics* **21,** 1291–1293
52. Nichols, J., and Rajagopalan, K. V. (2002) *J. Biol. Chem.* **277,** 24995–25000
53. Moulis, J., Davasse, V., Golinelli, M., Meyer, J., and Quincal, I. (1996) *J. Biol. Inorg. Chem.* **1,** 2–14